JTTEES 2:151-159

HVOF Combustion Spraying of Inconel Powder

D.J. Varacalle, Jr., M.G. Ortiz, C.S. Miller, T.J. Steeper, A.J. Rotolico, J. Nerz, and W.L. Riggs II

A major trend in the thermal spray industry has been to increase the gas jet velocity to obtain better coating attributes. One emerging technology now used in industry is the high-velocity oxygen fuel process (HVOF). High-velocity spray guns combine oxygen and a fuel gas to generate heat and extremely high particle velocities. In this study, Inconel 718 powder was deposited on steel substrates. The primary coating function was electrical resistivity for a heater application. Experiments were conducted using a Taguchi L8 statistical fractional/factorial design parametric study. The Taguchi experiment evaluated the effect of six HVOF processing variables on the measured responses. The parameters were oxygen flow, fuel flow, air envelope gas flow, powder feed rate, spray distance, and nozzle configuration. The coatings were characterized by hardness tests, surface profilometry, optical metallography, and image analysis. This article investigates coating hardness, porosity, surface roughness, deposition efficiency, and microstructure with respect to the influence of the processing parameters. Analytical studies were conducted to investigate gas, particle, and coating dynamics for two of the HVOF thermal spray experiments.

1. Introduction

THERMAL spray is a coating process used to apply metallic and nonmetallic coatings.[1] These processes are grouped into four major spray categories: plasma-arc, flame (combustion), electric-arc, and nozzle aspirated. Energy sources are used to heat the coating materials (i.e., in powder, wire, or rod form) to a molten or semimolten state. The resultant heated particles are accelerated and propelled toward a prepared surface by either process gases or atomization jets. Upon impact, a bond forms between the surface and the particles causing thickness buildup. In recent years, the major trend in the thermal spray industry has been to increase the powder particle velocity to obtain better coating attributes such as hardness, density, and wear resistance.

2. The HVOF Process

The high-velocity oxygen fuel (HVOF) process achieves extremely high particle velocities that result in enhanced coating properties for selected materials. The Metco high-velocity spray gun, designated the Diamond Jet (DJ), is capable of transferring kinetic and thermal energy to powder particles with a high degree of efficiency. The results of this process are high bond strength and density, as well as metallurgical structures that exhibit metalworking properties similar to those of wrought material.[2] With the relatively low flame temperatures (i.e., 3000 K, or 4940 °F) of the process, the feedstock material is softened by convective heat transfer with no super heating or vaporization of the particles. When the semimolten particles strike the substrate, their temperature peaks as the high kinetic energy of the particle is transformed into thermal energy.[3]

HVOF combustion temperatures and characteristics depend on the ratio and stoichiometry of the oxygen-fuel mixture. The ratio of fuel to oxygen is important in determining the final coating structure. Ideal stoichiometric combustion of propylene requires a 4.5:1 ratio of oxygen to fuel molecules ($2C_3H_6 + 9O_2 = 6H_2O + 6CO_2$). This combustion ratio produces a neutral flame (i.e., each oxygen and fuel molecule is consumed during combustion). If the combustion ratio is lean, unconsumed oxygen molecules in the flame create an oxidizing environment. This condition can result in excessive oxidation of molten metallic powder particles, leading to a high level of oxides in the coating. This depends on how lean the mixture is and on the type of metal. A fuel-rich mixture creates an oxygen-depleted reducing flame of low temperature, resulting in increased volume percentages of unmelted particles and porosity, but a low oxide content. In practice, the neutral flame does not exist. At high temperatures, the combustion process is not irreversible, and reactants and products coexist in thermal and chemical equilibrium. Early work by Hewitt[4] provides a more practical set of oxygen-fuel ratios, as they occur in industrial applications.

3. Application

Thermal spray processes are being used to fabricate heater tubes for use in thermal-hydraulic experiments to simulate nuclear fuel tubes.[5,6] These tubes are heated with a high-amperage, direct current power source to simulate nuclear fuel tube behavior. The heaters are fabricated using a multilayered coating system (metal bond coat, ceramic insulator, metal conductor, ceramic insulator, aluminum skin). The Inconel coating of this study is being considered for use as the conductor for the heater tubes. The coating used for this application must survive thermal cycling from thermal-hydraulic testing (which induces the tendency for spalling and cracking). It must match the prototypical heat storage and transfer of a nuclear fuel tube and also have the correct electrical resistivity to match the electrical power requirements. Former work in this area centered on the

Keywords: HVOF process, Inconel powder, Taguchi methodology, coating optimization, process modeling

D.J. Varacalle, Jr., M.G. Ortiz, and **C.S. Miller,** EG & G Idaho, Inc., Idaho National Engineering Laboratory, Idaho Falls, Idaho; **T.J. Steeper,** Westinghouse Savannah River Company, Savannah River Laboratory, Aiken, South Carolina; **A.J. Rotolico** and **J. Nerz,** Metco/Perkin Elmer, Westbury, New York; and **W. L. Riggs II,** TubalCain Company, Loveland, Ohio.

use of plasma-sprayed nickel-aluminum coatings for the conductor.[5]

The purpose of this article is to assess experimentally and analytically the important features of the HVOF spray system and to review the characteristic properties of the Inconel coatings. The results further the understanding of the physical mechanisms involved in the formation of metal coatings by systematically determining which HVOF processing parameters affect coating structure and properties.

4. Experimental Procedure

The Metco DJ combustion spray system was used for the experiments. This high-velocity spray process involves the continuous combustion of oxygen and a fuel gas within an air-cooled nozzle chamber, as shown in Fig. 1. After combustion, the hot gases are discharged, and the powder is fed axially and centrally into this exhaust gas stream. The flame is characterized by a high-velocity plume capable of accelerating the powder particles to high speeds. Depending on the feed pressures of the combustion gases, gas velocities exiting the nozzle can be on the order of 1200 m/s (3940 ft/s).[3]

A Taguchi-style, fractional-factorial L8 design of experiment[7] was used to evaluate the effect of six combustion processing variables on the quantitatively measured responses. The parameters varied were oxygen flow, fuel flow, air envelope gas flow, powder feed rate, spray distance, and nozzle configuration. Experiments IDJ1 through IDJ9 represent the nine runs evaluated with the Taguchi L8 approach, as detailed in Table 1. Each variable has two levels selected to band around the nominal settings (Experiment IDJ9) to demonstrate the combustion processing capabilities at a variety of stable combustion conditions.

Commercially available thermal spray powder (Metco Diamalloy 1006) was sprayed on 25.4 × 76.2 × 3.175 mm (1 × 3 × 0.125 in.) steel coupons for the experiments (Table 1). The Inconel 718 powder was fabricated using a water atomization process and was composed of nickel (52.5%), chromium (19%), iron (18.5%), cadmium (5.1%), molybdenum (3%), titanium (0.9%), aluminum (0.5%), manganese (0.2%), silicon (0.2%), and carbon (0.04%). The powder ranged in size from 10 to 62 μm. The fuel gas was propylene (C_3H_6). An x-y manipulator was used to fix the spray distance and ensure the repeatability of the experiments. The y-step was 1.59 mm (0.0625 in.). After the substrates were chemically cleaned and grit blasted, 8 to 27

Table 1 HVOF thermal spray experiments IDJ1 through IDJ9

Experiment	Oxygen flow			Fuel flow			Air flow			Feed rate		Spray		Hardware	
No.	FMR	scfh	scmh	FMR	scfh	scmh	FMR	scfh	scmh	kg/h	lb/h	mm	in.	(S/E)	Passes
IDJ1	44	635	18.0	30	132	3.7	47	742	21.0	1.36	3.0	203.2	8.0	S	9
IDJ2	44	635	18.0	30	132	3.7	54	852	24.1	2.73	6.0	304.8	12.0	E	9
IDJ3	44	635	18.0	43	184	5.2	47	742	21.0	1.36	3.0	304.8	12.0	E	9
IDJ4	44	635	18.0	43	184	5.2	54	852	24.1	2.73	6.0	203.2	8.0	S	9
IDJ5	52	750	25.1	30	132	3.7	47	742	21.0	2.73	6.0	203.2	8.0	E	9
IDJ6	52	750	25.1	30	132	3.7	54	852	24.1	1.36	3.0	304.8	12.0	S	8
IDJ7	52	750	25.1	43	184	5.2	47	742	21.0	2.73	6.0	304.8	12.0	S	8
IDJ8	52	750	25.1	43	184	5.2	54	852	24.1	1.36	3.0	203.2	8.0	E	9
IDJ9 (EMR)	46	664	18.8	43	184	5.2	50	788	22.3	1.36	3.0	254.0	10.0	S	27

Note: FMR = console flow meter reading, scfh = standard cubic feet per hour, scmh = standard cubic meters per hour, S = standard gun nozzle hardware, E = extended gun nozzle hardware, EMR = equipment manufacturers' recommended process parameters.

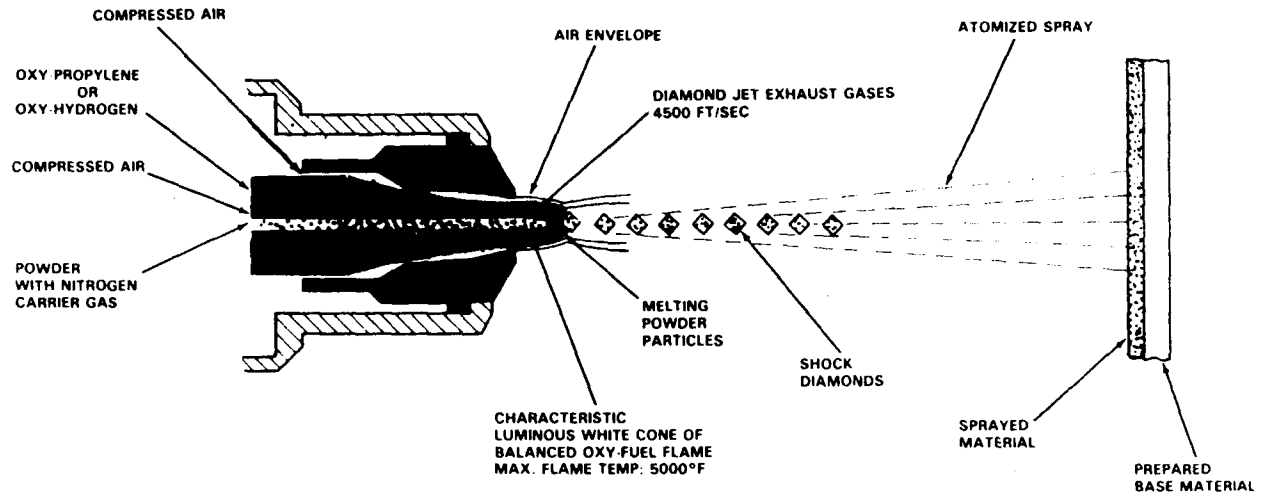

Fig. 1 Schematic cross section of Metco Diamond Jet spraying gun.

passes were used to fabricate each of the coatings shown in Table 1.

5. Combustion Dynamics

The temperatures and energy levels generated in the nine HVOF combustion experiments were calculated with the COMBUST code using the stoichiometry suggested by Hewitt,[4] in which CO is a major combustion product. The oxygen-to-fuel ratio required to satisfy complete combustion was 3:1. In these calculations, it was assumed that the reaction would be adiabatic and instantaneous. The reaction would begin and end in the combustion chamber, and any heat losses to the surroundings would be negligible. In reality, the reaction could reach beyond the combustion chamber, and heat losses could be significant. The solution required the initial flows of the reactants. The products of the reaction and the thermal properties of the mixture were calculated. Then, the heat generated by the reaction was calculated, and the adiabatic temperature and gun power were obtained with these results. Table 2 illustrates the results of the code predictions, including the mole fraction of the predicted products (i.e., CO, H_2, H, H_2O, O, N_2, O_2, CO_2, and OH).

The ratio of oxygen to fuel for all nine experiments exceeded Hewitt's value of 3:1. Thus, all experiments were fuel lean, resulting in complete combustion of the fuel and an oxygen-rich plume that tended to result in more oxidation of the metallic powder particles than would be observed at stoichiometric conditions. The temperature and energy values represent an upper bound, because in practice, heat losses occur and the reaction is carried beyond the combustion chamber into the free plume. The relative ranking (cooler or hotter) among the various experiments was expected to be more precise (i.e., IDJ3 produced the hottest gas mixture and IDJ6 the coolest). Combustion temperatures ranged from 2272 to 3057 K (3630 to 5043 °F). The amount of energy produced in the gas (i.e., power, as calculated using the heat of formations) was either 53.2 or 74.1 kW for the Taguchi experiments and 68.9 kW for the nominal process parameters (i.e., IDJ9). The primary combustion products were H_2O, CO, and H_2.

6. Materials Characterization Results

Table 3 lists the coating characterization results for this study. The coating attributes evaluated were thickness, superficial hardness, microhardness, porosity, oxide content, deposition efficiency, and surface roughness.

The coating thicknesses, as revealed by image analysis, are listed in Table 3. Average thickness per pass from five measurements of the Inconel layers ranged from 2.4 to 22.9 μm/pass, reflecting the influence of the various spraying parameters.

Porosity and oxide content for the coatings, as revealed by image analysis, are listed in Table 3. A Dapple image analyzer with a Nikon Epiphot metallograph was used for the metallurgical mounts. Image analysis procedures were first tested for sensitivity to parameter variation. The average porosity of the metal coatings ranged from 0.01 to 0.72%. The average oxide content

Table 2 Combustion predictions for HVOF thermal spray experiments IDJ1 through IDJ9

Experiment No.	Temperature, K	Power, kW	O_2/fuel ratio	Mole fraction of products								
				CO	H_2	H	H_2O	O	N_2	O_2	CO_2	OH
IDJ1	2499	53.2	5.82	0.149	0.062	0.036	0.170	0.013	0.317	0.162	0.053	0.036
IDJ2	2382	53.2	5.97	0.141	0.059	0.034	0.161	0.013	0.342	0.164	0.050	0.034
IDJ3	3057	74.1	4.18	0.186	0.078	0.045	0.213	0.017	0.284	0.061	0.067	0.045
IDJ4	2924	74.1	4.29	0.178	0.075	0.043	0.203	0.016	0.310	0.068	0.064	0.043
IDJ5	2377	53.2	6.69	0.141	0.059	0.034	0.161	0.013	0.299	0.208	0.050	0.034
IDJ6	2272	53.2	6.84	0.134	0.056	0.033	0.153	0.012	0.324	0.208	0.048	0.033
IDJ7	2918	74.1	4.81	0.177	0.075	0.043	0.203	0.016	0.271	0.109	0.063	0.043
IDJ8	2876	74.1	4.52	0.174	0.073	0.043	0.200	0.016	0.304	0.085	0.062	0.043
IDJ9	2965	68.9	4.38	0.180	0.076	0.044	0.207	0.016	0.292	0.076	0.065	0.044

Table 3 Coating characterization results for experiments IDJ1 through IDJ9

Experiment No.	Thickness, μm	Thickness/pass, μm	Hardness(a)	Hardness(b)	Porosity, %	Deposition efficiency, %	Oxides, %	Roughness, μm
IDJ1	165	18.33	73.4	332	0.15	67.0	6.4	3.84
IDJ2	206	22.89	75.7	335	0.25	66.0	13.2	3.37
IDJ3	106	11.78	67.1	371	0.72	76.0	21.2	3.00
IDJ4	142	15.78	71.6	356	0.72	73.0	2.4	3.92
IDJ5	189	21.00	76.2	355	0.07	75.0	21.2	3.57
IDJ6	19	2.38	54.4	350	0.50	19.0	0.0	3.34
IDJ7	151	18.88	73.0	344	0.35	65.0	9.8	3.47
IDJ8	121	13.44	74.2	378	0.01	78.0	18.2	2.95
IDJ9	359	13.30	76.1	331	0.66	73.0	3.2	3.97

(a) Superficial Rockwell 15N hardness. (b) Vickers microhardness (300-g load).

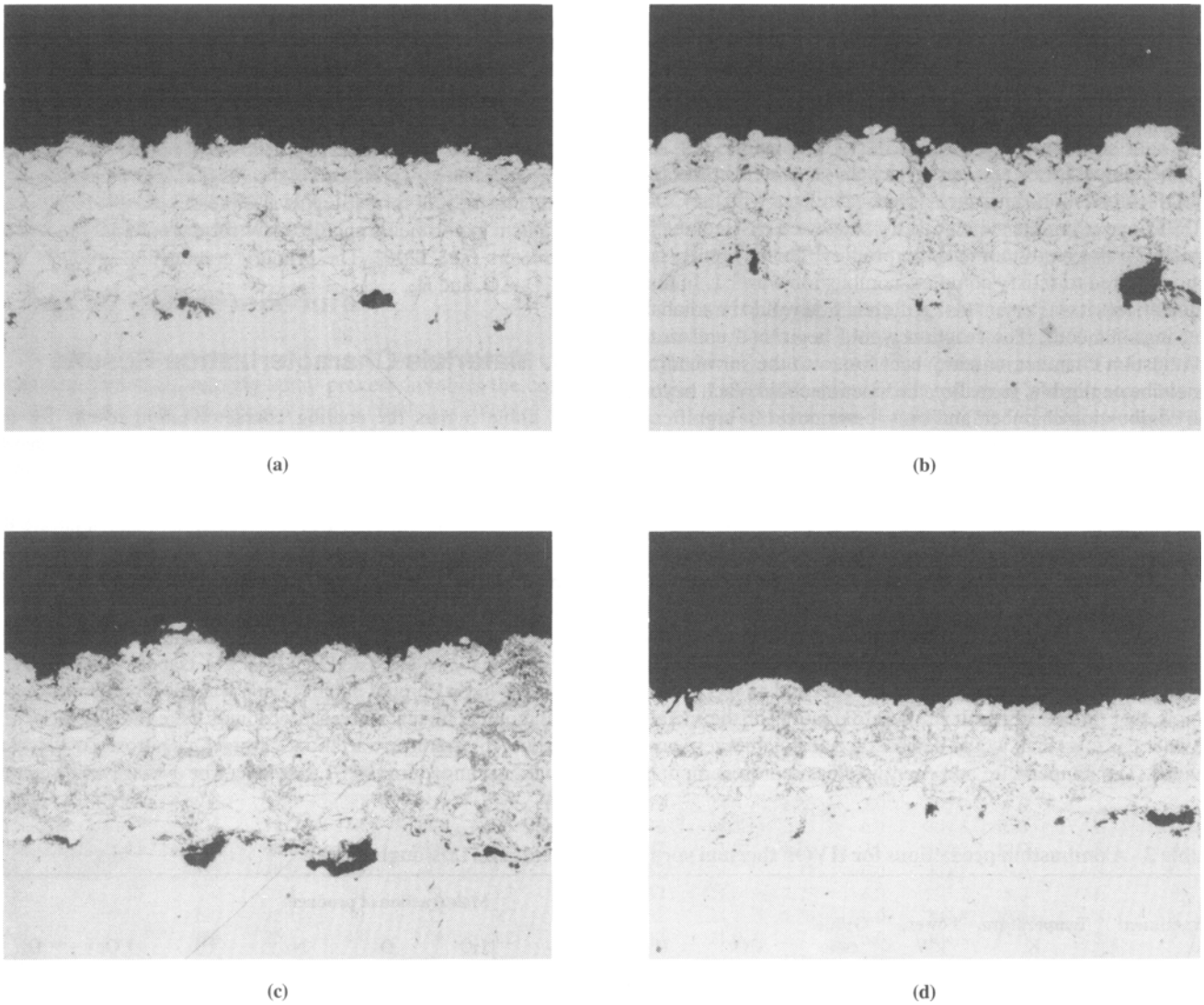

Fig. 2 Optical photomicrographs of as-sprayed coatings for experiments (a) IDJ1, (b) IDJ4, (c) IDJ5, and (d) IDJ8 (200×).

of the metal coatings ranged from 2.4 to 21.2%. This high oxide content is attributed to the fuel-lean mixture used in the experiments.

Superficial Rockwell hardness and Vickers microhardness measurements were taken on the coatings. The superficial Rockwell hardness measurement was taken normal to the deposit using the 15N method. Vickers microhardness measurements were taken on a cross section through the coating using a 300-g load. Five measurements were taken and averaged. Measurements for superficial hardness ranged from 54.4 to 76.2, whereas microhardness ranged from 331 to 378.

Deposition efficiencies for the ten experiments were determined using conventional techniques by measuring the amount of sprayed powder deposited for an allotted time. The deposition efficiencies ranged from 19 to 78%.

Surface roughness was determined using image analysis. The roughness of the coatings ranged from 3.0 to 4.0 μm. (Higher values are rougher.)

Image analysis revealed variances in the extent of porosity, oxides, and unmelted particles. Figures 2(a) through (d) illustrate microstructures for coatings IDJ1, IDJ4, IDJ5, and IDJ8. Experiments IDJ1 and IDJ5 were run at the 53.2-kW power level; experiments IDJ4 and IDJ8 were run at 74.1 kW. Coatings IDJ5 (Fig. 2c) and IDJ8 (Fig. 2d) exhibited the lowest porosity values of all coatings in this study. However, the oxide levels for these two coatings were the highest in the test series. Coating IDJ5 had a high percentage of unmelted particles in the matrix, whereas coating IDJ8 had practically no unmelted particles. Coatings IDJ1 (Fig. 2a) and IDJ4 (Fig. 2b) had the lowest oxide levels of all of the coatings, approximately five times lower than coatings IDJ5 and IDJ8. The porosity levels of these two coatings were still very low. Coating IDJ1 had the highest number of unmelted particles in the test matrix, whereas coating IDJ4 had approximately 66% of IDJ1. Coating IDJ1, shown in Fig. 2(a), may be the optimum coating of this study. Because the heater application for this study requires low resistivity, a coating with

Table 4 Results of the Taguchi analysis

Desired attributes	Processing factor						
	O_2 flow, ρ%/FMR	Propylene flow, ρ%/FMR	O_2X fuel, ρ%	Air flow, ρ%/FMR	Powder feed rate, ρ%/kg/h	Spray distance, ρ%/mm	Hardware, ρ%/S-E
Low porosity	1.5/52	0.6/30	9.3	21.7/47	13.6/1.36	1.0/203.2	52.2/E
Low oxides	0.9/44	3.0/30	0.2	16.0/54	0.0/1.36	0.4/304.8	79.4/S
High deposition efficiency	9.8/44	20.5/43	5.3	10.7/47	7.4/2.73	21.8/203.2	24.5/E
Low thickness/pass	7.3/52	1.0/43	21.7	10.2/54	45.2/1.36	6.8/304.8	8.0/S
High 15N Rockwell hardness	3.5/44	1.3/43	25.3	6.6/47	26.1/2.73	22.1/203.2	15.0/E
High Vickers hardness	7.5/52	40.8/43	12.7	2.0/54	11.6/1.36	3.0/203.2	22.4/E
High surface finish	9.5/44	8.8/30	0.5	1.3/47	20.8/2.73	17.6/203.2	41.5/S

Note: 15N = Rockwell 15N superficial hardness; FMR = console flow meter reading; S = standard nozzle hardware; E = extended nozzle hardware.

a combination of low porosity and low oxides may result in the best heater. Coating IDJ1 had a low porosity value, low oxide content, a high deposition efficiency, high intermediate hardness values, and a relatively rough finish.

7. Discussion of Taguchi Fractional-Factorial Experiment Design

Statistical design of experiment (SDE) strategies represent a method for constructively changing process parameters to determine their effect on the attributes of the product. A variety of SDE strategies are available (e.g., Box, Plackett and Burman, Box and Hunter, Taguchi) to obtain statistical information within the selected test matrix. The quantitative Taguchi evaluation of the HVOF thermal spray process is capable of displaying the range of measured coating characteristics attainable, and it statistically delineates the impact of each factor on the measured coating characteristics across all combinations of other factors. This information is useful in examining the physical science involved in thermal spray coatings, establishing realistic coating specifications, and developing new equipment. The Taguchi analysis was accomplished with personal computer-based software[8] on the measured responses.

The spray tests were conducted and evaluated once, and all data points were considered in the analysis of variance (ANOVA) calculations. The rho percent (ρ%) calculation indicates the influence of a factor or parameter on the measured response, with a larger number indicating more influence. The ANOVA calculations guide further experimentation by indicating which parameters are the most influential on coating attributes. Table 4 illustrates the results of the Taguchi analysis.

The Taguchi evaluation indicated that using the extended hardware was the most significant contributor to lowering porosity at 52.2 ρ%. Other contributors were air envelope flow at 21.7 ρ%, with the lower flow rate resulting in lower porosity and powder feed rate at 13.6 ρ%, with the lower powder feed rate resulting in lower porosity.

Oxide content was lowered using the standard hardware. This parameter at 79.4 ρ% completely dominated the other process variable contributions for this attribute. Deposition efficiency was increased by the use of the extended hardware (24.5 ρ%), shorter spray distance (21.8 ρ%), and higher propylene flow (20.5 ρ%). Coating thickness buildup increased with powder feed rate (i.e., 45.2 ρ%). Decreasing the powder feed rate will limit the thickness of the coating to acceptable requirements for the heater design.

Rockwell superficial hardness increased with higher powder feed rate (26.1 ρ%), and secondarily with shorter spray distance (22.1 ρ%). Vickers microhardness increased with higher fuel flow (40.8 ρ%) and the use of the extended nozzle hardware (22.4 ρ%). Surface roughness primarily increased with the use of the standard nozzle hardware (41.5 ρ%) and then secondarily with higher powder feed rate (20.8 ρ%) and shorter spray distance (17.6 ρ%).

The optimum coating would possess (as shown in Table 4 in order of priority) low porosity, low oxide content, high deposition efficiency, low thickness, high hardness, and a high (rough) surface finish for this particular application. This coating can be obtained by using a fuel flow of 5.2 scmh (184 scfh, 43 FMR), an oxygen flow of 18 scmh (635 scfh, 44 FMR), an air envelope gas flow of 21 scmh (742 scfh, 47 FMR), a powder feed rate of 1.36 kg/h (3 lb/h), a spray distance of 203.2 mm (8 in.), and the extended hardware. The process parameters for experiment IDJ1 used all the factor levels above with the exception of fuel flow and the standard hardware. Use of the standard hardware would tend to enhance the IDJ1 coating attributes in terms of lower porosity and higher deposition efficiency. The Taguchi evaluation used in this study should be used to develop specific confirmation runs that should approach optimum application attributes.

8. Analytical Modeling and Results

Modeling the combustion process for a thermal spray gun requires solving the conservation equations for both the gun nozzle (combustion region) and plume. The calculated flow and temperature fields are then used to solve gas/particle interaction in the free plume. The calculated molten state and velocity of the various particle sizes at the spray distance are then used in coating dynamics calculations. Experiments IDJ1 and IDJ4 were modeled in this study.

8.1 *Gas Dynamics Modeling and Results*

The CONCOM computer code calculates the exit conditions in a convergent nozzle combustion gun using C_3H_6 as a fuel. The input to the code involves combustion product flow rates,

Table 5 Temperature and velocity analytical results at a plume radial location 2 mm

Experiment No.	Nozzle exit		Midplane(a)		Spray distance	
	T	*v*	*T*	*v*	*T*	*v*
IDJ1	2499	1051	2425	1010	2305	996
IDJ4	2924	1165	2826	1117	2789	1100

Note: Temperature (*T*) in K; velocity (*v*) in m/s. (a) Midplane of plume is 0.102 m from nozzle exit.

Table 6 PROCESS particle dynamics results at spray distance for Inconel powder

Particle size, μm	wt%	IDJI Temperature, K	IDJI Velocity, m/s	IDJI Location, mm	IDJ4 Temperature, K	IDJ4 Velocity, m/s	IDJ4 Location, mm
11	3.3	2470	573	0.9	2825	618	0.9
14	3.4	2468	515	1.1	2840	554	1.1
16	14.0	2464	487	1.2	2840	523	1.1
19	10.6	2450	452	1.3	2842	479	1.2
22	23.5	2416	426	1.4	2842	448	1.4
26	12.9	2276	393	1.5	2834	412	1.5
31	18.6	1939	359	1.6	2811	378	1.6
38	5.6	1604	329	1.8	2738	345	1.8
44	6.4	1533	309	1.9	2626	323	1.9
53	0.8	1465	283	2.0	2347	297	2.0
62	0.9	1418	265	2.1	1970	276	2.1

specific heat of the mixture, combustion temperature, stagnation pressure, and nozzle geometry. It is assumed that the mixing and combustion take place in the converging nozzle, the combustion temperature occurs at the exit plane of the nozzle, the nozzle chokes (i.e., Mach number = 1.0), and the combustion products act as a perfect gas. The code calculates a mass-weighted gas constant, the gas-specific heat ratio, the exit velocity, mixture pressure, and gas density.

Table 5 illustrates the CONCOM-predicted centerline, gas temperature, and velocity at the nozzle exit for experiments IDJ1 and IDJ4. The gas temperature and velocity for experiment IDJ1 are predicted to be 2499 K (4038 °F) and 1051 m/s (3447 ft/s), whereas experiment IDJ4 is predicted to be 2924 K (4803 °F) and 1165 m/s (3821 ft/s).

The mass, momentum, and energy conservation equations were solved in the plume using TORCH,[5] a two-dimensional axisymmetric model. This code is an incompressible model that does not address shock dynamics. The code uses the output generated by CONCOM at the nozzle exit and calculates the plume gas dynamics. The input to the code involves transport and thermodynamic gas properties, the torch geometry, and the system operation parameters. Typical output from the plume dynamics model includes temperature, enthalpy, velocity, and viscosity profiles as a function of radial and axial position. Details, equations, input, and methodology for the model are discussed in Ref 9.

Results of the TORCH calculations are illustrated in Table 5 for a radial location of 2 mm in the plume at midplane and at the spray distance. The particles were predicted (see next section) to remain within 2.1 mm of the plume centerline for both experiments. As shown, at the nozzle exit plane, there was a 425 K (275 °F) difference in gas temperature and a 114 m/s (374 ft/s) difference in gas velocity between the IDJ1 (53.2-kW) and IDJ4 (74.1-kW) calculations. As shown in Table 5, the particle temperatures and velocities did not change substantially in this core region of the plume. The axial temperature and velocity gradients from the nozzle exit to the spray distance were 194 K (349 °F) and 55 m/s (180 ft/s) for IDJ1, and 135 K (243 °F) and 65 m/s (213 ft/s) for IDJ4. Thus, this region of the plume is optimum for gas/particle interaction. Outside a plume radius of approximately 4 mm, the plume interacts strongly with the ambient air, substantially reducing both the gas temperature and velocity.

8.2 *Particle Dynamics Modeling and Results*

The PROCESS[9] gas/particle computer program used in this study uses the temperature and velocity fields generated by the TORCH program to calculate the dynamics of particles injected into the plume. The primary result of the gas/particle code is a description of the injected particle vaporization rate, average temperature, and velocity as a function of position in the plume.

The specified initial conditions for the injected particles are the injection location, velocity, diameter, sphericity, and temperature. Also specified are the particle material properties, including density, specific heat, melting temperature, boiling temperature, heat of fusion, heat of vaporization, and emissivity. Details, equations, input, and methodology for the model are discussed in Ref 9.

Calculations were performed for Inconel powder particle diameters of 11, 14, 16, 19, 22, 26, 31, 38, 44, 53, and 62 μm to study gas/particle interaction for the two experiments. These sizes correspond to the measured Microtrac size distribution for Inconel shown in Table 6. Table 6 also lists the calculated particle temperature, velocity, and radial location from centerline in the plume at the spray distance for experiments IDJ1 and IDJ4.

Inconel 718 powder begins melting at 1533 K (2300 °F) and boils at 2956 K (4861 °F). For calculation IDJ1, all particles

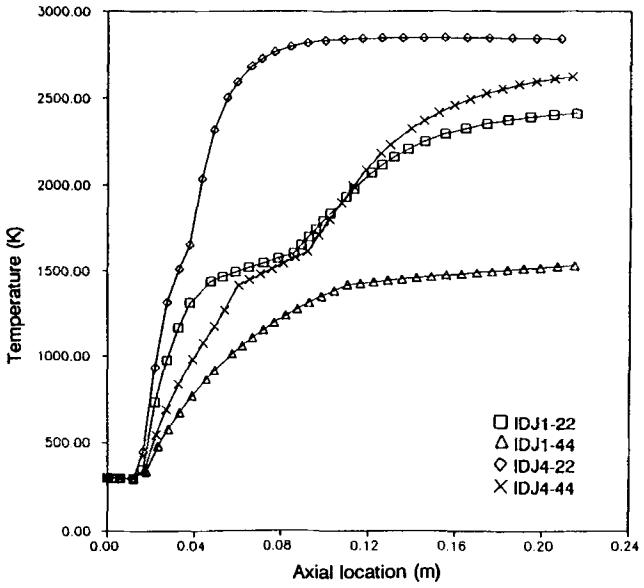

Fig. 3 Predicted particle temperatures for experiments IDJ1 and IDJ4.

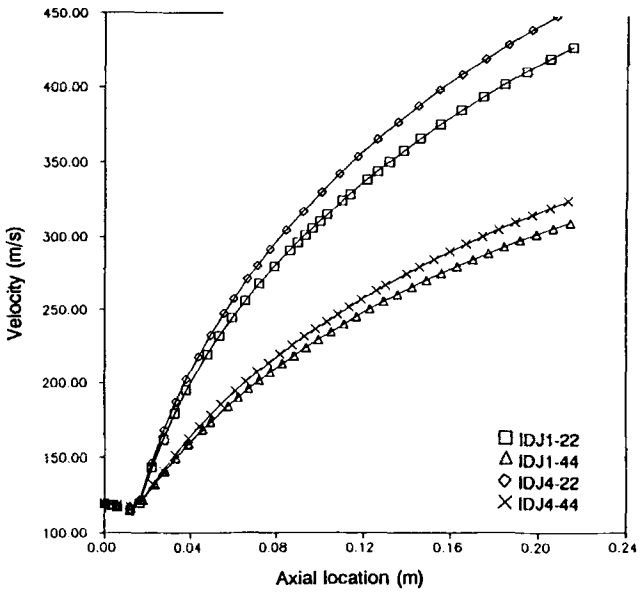

Fig. 4 Predicted particle velocities for experiments IDJ1 and IDJ4.

Table 7 BUILD coating dynamics results

Experiment No.	Measured Tk	Measured P	Measured DE	Calculated Tk	Calculated P	Calculated DE
IDJ1	165	0.15	67	177	1.6	69
IDJ4	142	0.72	73	191	0.7	94

Note: Tk = coating thickness in m; P = percent porosity; DE = input deposition efficiency in percent.

smaller than 44 μm were predicted to exceed the melting point of Inconel at the 203.2 mm (8 in.) spray distance. As illustrated for calculation IDJ4, all particles exceeded the melting point at the same spray distance. The particle temperatures for experiment IDJ4 were predicted to be substantially higher than the corresponding particle temperatures for IDJ1. This suggests that all of the particles for experiment IDJ4 were highly molten at the spray distance, whereas the larger (>38 μm) particles for experiment IDJ1 are not melted and would contribute a substantial amount of unmelted particles in the coating matrix. The calculations indicate that the smaller the particle, the higher the velocity at spray because of the larger acceleration from the drag forces. The velocities for the particles are extremely high because they follow the gas velocity trends. Because centerline injection was used and modeled in these experiments, the Inconel particles do not traverse far from the plume centerline (i.e., 2.1 mm maximum).

Figures 3 and 4 illustrate the predictions of particle temperature and velocity as a function of axial location in the plasma plume for 22- and 44-μm diameter particles for the two experiments. As shown, the predicted particle temperatures and velocities for the two cases exhibit the same trend: to increase throughout the trajectory as a result of the almost constant energy source in the center of the plume. The IDJ4 particles are predicted to be at substantially higher temperatures than the corresponding IDJ1 particles throughout the trajectory because of the difference in power levels between the two experiments, which is verified in Fig. 3. The predicted combination of highly molten conditions and high velocity for the particles results in high deposition efficiency and low porosity, as verified in Table 3 for the two coatings.

9. Coating Dynamics Modeling and Results

The BUILD coating dynamics computer program[10] used in this study uses the particle output generated by the PROCESS code at the spray distance to calculate the dynamics of the coating buildup. The code calculates the morphology of the injected particles one at a time and accumulates the results. The code calculates the coating thickness, porosity, and the average temperature and velocity of the impacting particles in the coating matrix. The specified initial conditions for the BUILD code are the particle location in the free plume, velocity, temperature, diameter, and weight percentage of that particle diameter family. Also specified are the powder material properties (i.e., density, specific heat, melting temperature, boiling temperature, and viscosity as a function of temperature) and the process parameters (i.e., powder feed rate, powder deposition efficiency, traverse rate, number of passes, number of traverses, y-step). Details, equations, input, and methodology for the model are discussed in Ref 8.

Using the PROCESS calculations for the Inconel particles, a particle plume distribution was established for each experiment to study coating morphology as a function of the various process parameters. Table 7 illustrates the calculated coating dynamics results. The calculated thickness is a strong function of the deposition efficiency (DE). As shown for IDJ1, the thickness and deposition efficiency predictions were very accurate, and the porosity calculation was reasonably accurate. For IDJ4, the porosity prediction was very accurate, and the thickness calculation was reasonably accurate. This correlation is attributable to the predicted temperatures of the particles. The IDJ1 temperature predictions for the larger particles were too low, whereas the IDJ4 particle temperature predictions were too high. The DE prediction for IDJ4 was too high, which is attributed to the high predicted temperatures of the particles.

The higher predicted temperatures and velocities for experiment IDJ4 relative to experiment IDJ1 would result in higher deposition efficiency, lower oxide content resulting from decreased particle residence time, higher microhardness, and lower porosity. Characterization results shown in Table 3 correlate with these observations except for porosity. However, the variance in the measured porosities would tend to favor these conclusions.

10. Summary and Conclusions

An analytical and experimental study of the HVOF combustion spraying of Inconel powder has been presented. Experiments used a Taguchi fractional-factorial approach with typical process parameters. The coatings were characterized by hardness tests, surface roughness, image analysis, and optical metallography. Coating qualities were determined for hardness, roughness, deposition efficiency, and microstructure.

The Inconel coating thicknesses per pass, reflecting the influence of the spraying parameters, ranged from 2.4 to 22.9 μm. Porosity for the coatings, as revealed by image analysis, ranged from 0.04 to 0.72%. Oxide content in the coatings, as revealed by image analysis, ranged from 3.2 to 21.2%. Measurements for superficial Rockwell hardnesses ranged from 54.4 to 76.2, whereas the microhardness measurements ranged from 331 to 378. The roughness of the coatings ranged from 2.95 to 3.97 μm. Deposition efficiencies ranged from 19 to 78%. For the application of this study, coating IDJ1 was the best coating produced.

The Taguchi evaluation indicated that use of the extended hardware contributed most to lowering porosity. Oxide content was lowered by using the standard hardware. Deposition efficiency was increased by use of the extended hardware, shorter spray distance, and higher propylene flow. Coating thickness buildup was predominantly a function of powder feed rate. Rockwell superficial hardness was increased primarily by the higher powder feed rate and secondarily by shorter spray distance. Vickers microhardness increased primarily by the higher fuel flow and secondarily by the use of the extended nozzle hardware. Surface roughness increased with the use of the standard nozzle hardware.

An optimum coating for this particular application can be obtained by using a fuel flow of 5.2 scmh (184 scfh), an oxygen flow of 18 scmh (635 scfh), an air envelope gas flow of 21 scmh (742 scfh), a powder feed rate of 1.36 kg/h (3 lb/h), a spray distance of 203.2 mm (8 in.), and the extended hardware. These process parameters would enhance the coating attributes for coating IDJ1, the best coating produced in this study.

The calculation methods used in this article present a first approximation to interpreting the HVOF process. The gas dynamics numerical calculations illustrate reasonable quantitative trends of the gas dynamics in commercial HVOF spray guns, for power levels of 53.2 and 74.1 kW. Computer simulations of the particle dynamics of 11- to 62-μm Inconel particles indicate that most of the particles were molten at the spray distance. The coating dynamics code reasonably predicted the thickness, porosity, and deposition efficiency of the coatings for the two modeled experiments and indicated correlation with the coating oxide contents and microhardnesses.

The objective of this and future work is to optimize thermally sprayed coatings. The procedure described in this article will assist in selecting and optimizing operational parameters for future HVOF experiments and applications.

Acknowledgments

The work described in this article was supported by the US Department of Energy, Assistant Secretary for Defense, under DOE Idaho Field Office Contract No. DE-AC07-76ID01570.

References

1. E.J. Kubel, Thermal Spraying Technology: From Art to Science, *Adv. Mater. Proc.*, Vol 132 (No. 6), Dec 1987, p 69-80
2. D.W. Parker and G.L. Kutner, HVOF—Spray Technology—Poised for Growth, *Adv. Mater. Proc.*, Vol 139, Apr 1991, p 68-74
3. R.W. Kaufold, A.J. Rotolico, J.E. Nerz, and B.A. Kushner, Deposition of Coatings Using a New High Velocity Combustion Spray Gun, *Thermal Spray Research and Applications*, T.F. Bernecki, Ed., ASM International, 1991, p 561-569
4. A.D. Hewitt, Technology of Oxyfuel Gas Processes, *Weld. Met. Fabr.*, Nov 1972, p 382-389
5. T.J. Steeper, D.J. Varacalle, Jr., G.C. Wilson, and V.T. Berta, Use of Thermal Spray Processes to Fabricate Heater Tubes for Use in Thermal-Hydraulic Experiments, *Thermal Spray Coatings: Properties, Processes, and Applications*, T.F. Bernecki, Ed., ASM International, 1991, p 425-432
6. T.J. Steeper, D.J. Varacalle, Jr., G.C. Wilson, A.J. Rotolico, J.E. Nerz, and W.L. Riggs, A Taguchi Experimental Design Study of Plasma Sprayed Alumina-Titania Coatings, *Thermal Spray Coatings: Properties, Processes, and Applications*, T.F. Bernecki, Ed., ASM International, 1991, p 13-20
7. G. Taguchi and S. Konishi, *Taguchi Methods: Orthogonal Arrays and Linear Graphs*, ASI Press, 1987
8. R.F. Culp, "Speedy Analysis and Design of Industrial Experiments," (SADIE), GE Medical Systems, Milwaukee, 1990
9. Y.C. Lee, "Modeling Work in Thermal Plasma Processing," Ph.D. thesis, University of Minnesota, Minneapolis, 1984; available from University Microfilms International, DER84-24718
10. D.J. Varacalle, Jr., An Analytical Methodology to Predict the Coating Characteristics of Plasma-Sprayed Ceramic Powders, *Thermal Spray Research and Applications*, T.F. Bernecki, Ed., ASM International, 1991, p 271-283